Fertility and Sterility

Comparison of different sources of platelet-rich plasma as treatment option for infertility-causing endometrial pathologies

--Manuscript Draft--

Manuscript Number:	FandS30507R2
Article Type:	Reproductive Biology
Keywords:	Asherman's Syndrome; Endometrial Atrophy; platelet-rich plasma; umbilical cord blood; Regenerative Medicine
Corresponding Author:	Irene Cervello, PhD Fundación Instituto Valenciano de Infertilidad (FIVI), Instituto Universitario IVI/INCLIVA, Valencia, Spain. Valencia, SPAIN
First Author:	Lucía de Miguel-Gómez, M.Sc.
Order of Authors:	Lucía de Miguel-Gómez, M.Sc.
	Sara López-Martínez, M.Sc.
	Hannes Campo, Ph.D.
	Emilio Francés-Herrero, B.Sc.
	Amparo Faus, B.Sc.
	Ana Díaz, Ph.D.
	Antonio Pellicer, M.D., Ph.D.
	Francisco Domínguez, Ph.D.
	Irene Cervello, PhD
Abstract:	Objective. To study the effect of human plasma from different sources such as umbilical cord blood and adult blood platelet-rich plasma (PRP) on the regeneration of endometrial damage. Design. Composition analysis, in vitro approaches and a pre-clinical murine model using plasma to promote endometrial regeneration. Setting. Hospital and university laboratories. Patients/Animals. Adult plasma from 4 Asherman's Syndrome/Endometrial Atrophy patients and one fertile woman, commercial umbilical cord plasma and uterine-damaged NOD/SCID mice model were used. Intervention(s). Endometrial stromal cells from primary culture and an endometrial stem cell line were cultured in vitro and uterine-damaged NOD/SCID mice were treated with plasma samples from several origins. Main Outcome Measure(s). All plasma samples contain molecules with a high potential for regeneration (SCF, PDGFBB, THBS1, VWF). Furthermore, the highest increase in in vitro proliferation and migration rate was found when endometrial stromal cells were treated with umbilical cord plasma, adult PRP also revealed a significant increment. In the mouse model, a higher expression of Ki67 and Hoxa10 in the endometrium was detected after applying adult PRP and the proteomic analysis revealed a specific protein expression profile depending on the treatment. The damaged uterine tissue showed more pro-regenerative markers after applying umbilical cord plasma (Stat5a, Uba3, Thy1) in comparison to the other treatments (non-activated umbilical cord plasma, activated adult PRP and not treatment). Conclusion. Human PRP possesses regeneration properties usable for endometrial pathologies. Besides that, these regenerative effects seem to be more apparent when the source of obtaining is umbilical cord blood.

Running title: Endometrial regeneration using plasma

Title: Comparison of different sources of platelet-rich plasma as treatment option for infertility-causing endometrial pathologies

Authors: Lucía de Miguel-Gómez, M.Sc.,[a,b] Sara López-Martínez, M.Sc.,[a] Hannes Campo, Ph.D.,[a] Emilio Francés-Herrero, B.Sc.[a,b] Amparo Faus, B.Sc.,[a] Ana Díaz, Ph.D.,[b] Antonio Pellicer, M.D., Ph.D.,[c,] Francisco Domínguez, Ph.D.,[a] Irene Cervelló, Ph.D.,[a].

FD and IC should be considered as joint last authors.

a. Fundación Instituto Valenciano de Infertilidad (FIVI), Instituto de Investigación Sanitaria La Fe, Valencia, Spain.
b. University of Valencia, Spain.
c. IVIRMA Roma, Italy.

Correspondence:

Irene Cervelló

Fundación Instituto Valenciano de Infertilidad (FIVI), Instituto de Investigación Sanitaria La Fe, Avenida Fernando Abril Martorell, 106. Hospital La Fe, Torre A, Planta 1ª, Valencia 46026, Spain.

Email: Irene.cervello@ivirma.com

Capsule: According to a composition analysis, i*n vitro* and *in vivo* assays, platelet-rich plasma seems to be a promising option for enhancing endometrial regeneration, especially when coming from umbilical cord blood.

ABSTRACT

Objective. To study the effect of human plasma from different sources such as umbilical cord blood and adult blood platelet-rich plasma (PRP) on the regeneration of endometrial damage.

Design. Composition analysis, *in vitro* approaches and a pre-clinical murine model using plasma to promote endometrial regeneration.

Setting. Hospital and university laboratories.

Patients/Animals. Adult plasma from 4 Asherman's Syndrome/Endometrial Atrophy patients and one fertile woman, commercial umbilical cord plasma and uterine-damaged NOD/SCID mice model were used.

Intervention(s). Endometrial stromal cells from primary culture and an endometrial stem cell line were cultured *in vitro* and uterine-damaged NOD/SCID mice were treated with plasma samples from several origins.

Main Outcome Measure(s). All plasma samples contain molecules with a high potential for regeneration (SCF, PDGFBB, THBS1, VWF). Furthermore, the highest increase in *in vitro* proliferation and migration rate was found when endometrial stromal cells were treated with umbilical cord plasma, adult PRP also revealed a significant increment. In the mouse model, a higher expression of Ki67 and Hoxa10 in the endometrium was detected after applying adult PRP and the proteomic analysis revealed a specific protein expression profile depending on the treatment. The damaged uterine tissue showed more pro-regenerative markers after applying umbilical cord plasma (Stat5a, Uba3, Thy1) in comparison to the other treatments (non-activated umbilical cord plasma, activated adult PRP and not treatment).

Conclusion. Human PRP possesses regeneration properties usable for endometrial pathologies. Besides that, these regenerative effects seem to be more apparent when the source of obtaining is umbilical cord blood.

Keywords: Asherman's Syndrome, Endometrial Atrophy, platelet-rich plasma, umbilical cord blood, Regenerative Medicine.

INTRODUCTION

The endometrium is an extremely regenerative and complex tissue lining the uterus. It is responsible for embryo implantation and the success of the future pregnancy during the female reproductive life (1,2). However, some disorders affecting this tissue can complicate the implantation process (3–5). In this context, Asherman's Syndrome (AS) and Endometrial Atrophy (EA) are relevant endometrial pathologies causing these types of fertility problems. AS is defined by the presence of intrauterine adhesions, which contribute to a partial or complete absence of functional endometrium (6), while EA is characterized by insufficient endometrial growth (7). Women suffering from AS or EA have a lower probability of a successful pregnancy because of impaired implantation and early abortion (8). However, until now, there has not been a completely effective and reliable therapy. Different treatments have been proposed (7), but only stem cell therapy has shown any effectiveness (9–14). Nevertheless, this kind of treatment implies invasive and expensive procedures. For this reason, the medical and scientific community is still looking for alternative and cost-effective therapies. In the last years, platelet-rich plasma (PRP) has been proposed as a promising alternative: PRP can easily be isolated and applied non-invasively and moreover this can be done autologously.

Over the last two decades, PRP has been used in different medical fields ranging from dermatology to dental surgery (15–17). PRP is a plasma fraction with a platelet concentration above the normal average (~200.000 platelets/µl) (18). It is known that platelet α-granules deliver, after activation, cytokines, chemokines, and different growth factors such as platelet-derived growth factor (PDGF), vascular endothelial growth factor (VEGF), hepatocyte growth factor

(HGF), transforming growth factor beta (TGFβ), or stromal cell-derived factor 1 alpha (SDF1α). Therefore, PRP is enriched in these factors (18,19), which play a crucial role in the recruitment of different cell types that proliferate and migrate towards the injured site, promoting tissue regeneration and angiogenesis (18,20).

More recently, PRP has started to be used in reproductive medicine. Different groups have shown positive results using *in vitro* experiments using human endometrial cells (21–23). Furthermore, rodent models have also shown promising results, describing how PRP administration in damaged uterine horns enhances cell proliferation, reduces fibrosis, and even increases implantation sites (24,25). Some "proof of concepts" in humans have been carried out too, instilling autologous PRP in patients with a thin endometrium (26–28). However, there is still a need for a profound understanding of its mechanism of action.

Going one step forward, PRP can be obtained not only from adult peripheral blood, but also from umbilical cord blood (UCB). It has been generally considered that the younger the source, the higher its regenerative potential is. It is thought to be linked to the higher concentration of growth and pro-angiogenic factors found in comparison to plasma from an older source (29). This has been illustrated functionally using *in vitro* (30,31) and *in vivo* (32,33) assays. There are also several ongoing clinical trials using umbilical cord PRP (34–36).

In this pilot study, we developed novel *in vitro* and *in vivo* models to investigate the possible beneficial effects of PRP from AS/EA patients. Using both approaches we aimed to compare if plasma from human UCB had a stronger effect than adult PRP in promoting pro-regenerative events in endometrial

afflictions. We also aimed to ensure that PRP from AS/EA patients was as effective as the one from a healthy woman and thus could be used for autologous treatment.

MATERIAL AND METHODS

Study design

An overview of our study is detailed in Figure 1. After extracting peripheral blood (PB) from patients with endometrial pathologies (n=4) and a control (fertile female, n=1), PRP was prepared (Figure 1A). Commercial umbilical cord plasma (STEMCELL Technologies, Catalog #70020.2, Lot. #1706230142) was also prepared (Figure 1B). The product information we received revealed a female Caucasian donor who tested negative for HIV-1 and 2, and Hepatitis B and C. The product was obtained using consent forms and protocols approved by either the Food and Drug Administration or an Institutional Review Board. Part of these samples were activated with 0.1 M calcium chloride ($CaCl_2$) (Sigma Aldrich, Catalog #21115), for inducing platelet degranulation and growth factors and other signaling molecules secretion. Then, samples were used for 3 different experiments (Figure 1B). First, Liquid Chromatography coupled to Mass Spectrometry (LC-MS/MS) and multiplex protein immunoassays were used for analyzing the specific plasma composition. Secondly, an *in vitro* approach for measuring cell proliferation and migration was developed to demonstrate the plasma effect over key cellular processes involved in tissue regeneration. Finally, an Asherman Syndrome (AS) murine model was employed, where the uterine horns were analyzed by Sequential Window Acquisition of All Theoretical-Mass Spectra (SWATH-MS) to evaluate if plasma was able to recover damaged uterine horns.

Human plasma samples and PRP preparation

PB samples were collected from 4 different AS/EA patients (diagnosed by hysteroscopy in proliferative phase) and from a female control, with proven

fertility; all of them aged between 34 and 49 provided informed consent. This study was approved by the Clinical Ethics Committee of IVI Valencia (1707-FIVI-003-IC).

To isolate PRP, all PB samples were sequentially centrifuged (280g/8min/RT followed by 400g/15min/RT) and the PRP (upper part) and platelet-poor plasma (PPP, lower part) fractions were collected (Figure 1A). Then, all patient samples (aPRP), part of the PRP control (aPRPC) and part of the umbilical cord plasma (aUCP) were activated using 5% of $CaCl_2$ 0.1 M.

Adult PRP and UCP analysis by proteomic analysis

LC-MS/MS technique was performed as described elsewhere (37). Briefly, all samples were loaded into a 1D SDS-PAGE gel and LC-MS/MS analysis was performed, eluted peptides were analyzed in a nanoESI qQTOF mass spectrometer and all the fragments were combined in a single search using ProteinPilot v.5.0 and the Swissprot database.

Two immunoassays, covering 46 different analytes (Supplemental Table 1), were performed in all samples: Cytokine/Chemokine/Growth Factor 45-Plex Human ProcartaPlex™ Panel 1 and TGF-B1 Human ProcartaPlex™ Simplex Kit (Thermo Fisher Scientific, catalog #EPX450-12171-901 and #EPX01A-10249-901). Quantification was carried out using a Luminex MagPix system and Luminex xPonent Software.

In vitro evaluation of cell proliferation and migration assays

Both assays were performed with two different cell types: a human stromal stem cell line, ICE7 (n=3), obtained by using Hoescht methodology previously described (1); and primary human endometrial stromal cells (hESCs) obtained

from endometrial biopsies from healthy oocyte donors (n=10) (38). In both assays, 3 conditions (No Treatment, aPRP and aUCP) were studied. Furthermore, in the cell proliferation assay using ICE7 cells we performed some preliminary tests: 3 more conditions were included (aPRPC, naPRPC and aPPP) to check the optimal concentration (1%, 5%, 10% or 20%) of treatment in the culture media.

For viable cell proliferation assay, cells were seeded in a 96-well plate and incubated overnight with DMEM supplemented with 10% fetal bovine serum (FBS). Thereafter, CellTiter 96® AQueous One Solution Reagent (Promega, catalog #G3580), containing a tetrazolium compound (MTS), was added and absorbance (490nm) was measured to evaluate viable cell proliferation.

For the wound healing assay, cells were seeded in 24-well plates with DMEM supplemented with 10% FBS and grown to confluence. The monolayer was then scratched using a pipette tip. After washing the wells with phosphate-buffered saline solution for removing detached cells, corresponding treatments were added and cells were photographed 0, 24 and 48 hours after scratching and the wound area was quantified using Image J software.

In vivo experiments: proteomic profiles and endometrial regeneration in an AS animal model

In vivo procedures were performed in female eight-week-old NOD-SCID mice (Charles River Laboratories), according to the Ethics Committee for Animal Welfare (A1483088947170) of the University of Valencia (Spain). An adaptation from our previous protocol (12) was followed: damage was induced inside the lumen of left uterine horns (damaged) using a needle; right horns were left

undamaged (control). Mice were distributed in 4 groups and all of them underwent the same protocol: 3 successive injections (day 0, 2 and 4) through the tail vein, containing 100 µL of plasma each, and they were euthanized on day 7 (Figure 1B). The four groups were: No treatment group (n=6, milliQ H_20), naUCP group (n=6), aUCP group (n=6) and aPRP group (n=9). Mice from the last group were treated with aPRP from 4 different patients (3 aPRP were injected in 2 animals each for SWATH-MS and the fourth aPRP, in the remaining animals). Endometrial tissue from both horns of 6 mice/group (n=48) was analyzed by SWATH-MS. We used the remaining mice (n=3) from aPRP group for a preliminary test before proceeding with the SWATH-MS analysis. Moreover, endometrial tissues were tested for Ki-67 (a cell proliferation marker) and Hoxa10 (a transcription factor directly related to endometrium function and development) signals, to demonstrate the pro-regenerative events.

Ki67 signal (1:100, Abcam, catalog #ab833) was measured by immunohistochemistry and Hoxa10 by Western Blot (WB) (1:100 SantaCruz, catalog #sc-281428). Image ProPlus (Media Cybernetics) and ImageJ software were respectively used for quantification.

Relative quantification of murine protein endometrial tissues by SWATH

SWATH-MS procedure was carried out as described elsewhere (39). Briefly, all samples were pooled to build the spectral library from a 1D SDS-PAGE gel, and resulting peptides were analyzed in a nanoESI qQTOF mass spectrometer. Then, tripleTOF was operated in SWATH mode for individual samples. Data were analyzed using Peak View 2.1 and Marker View. Protein areas were normalized by the total sum of the areas of all the quantified proteins. After statistical analysis, results were validated by WB.

Functional in silico analysis

For proteomic data analysis, Gene Ontology (GO) (40) and Kyoto Encyclopedia of Genes and Genomes (KEGG) (41) databases were considered through g:Profiler tool set (42), Genemania (43) and, 'KEGG mapper–Search pathway' web tools.

Statistical analysis

Data were analyzed using GraphPad Prism 7.04 software and presented as mean + standard deviation (SD) or median ± interquartile range (IQR), when required. An analysis of variance was used to analyze cell proliferation and wound closure rates and growth factors/cytokine/chemokine concentrations. A Mann Whitney test was used to analyze Ki67 and Hoxa10 signals. $P<0.05$ was considered statistically significant.

SWATH-MS data were analyzed using multinomial regression with Elastic Net penalization (Elastic Net penalty value, $\alpha=0.5$) (44).

RESULTS

Comprehensive proteomic evaluation of plasma from different sources

The LC-MS/MS proteomic analysis showed the presence of 616 proteins in aUCP, 331 in naUCP and 237 in aPRP samples. Only proteins detected in at least 2 of the aPRP samples were considered (Figure 2A). The functional *in silico* analysis revealed no relevant differences among PRP from patients and control (data not included), revealing that plasma from AS/EA patients is not different from a healthy woman and could be used as autologous treatment.

According to the objective of this study, we were interested in proteins related to tissue regeneration (45,46), specifically those localized inside platelet α-granules. Among all the proteins detected, thrombospondin-1 (THBS1), α-2-macroglobulin (A2M), von Willebrand factor (VWF), neural cell adhesion molecule 1 (NCAM1), or insulin-like growth factor II (IGF2) were found in all plasma samples. Meanwhile, other interesting proteins such as CD109 antigen, insulin-like growth factor-binding protein 4 (IGFBP4), and angiopoietin-related protein 3 (ANGPTL3) were detected only in naUCP; multimerin-1 (MMRN1), pyruvate kinase (PKM) and peroxiredoxin-1 (PRDX1) were exclusively found in aUCP. Finally, adenosine deaminase 2 (ADA2), 14-3-3 protein gamma (YWHAG), and macrophage migration inhibitory factor (MIF) were only found in aPRP (Figure 2A). To note that due to the big difference between aUCP and naUCP composition, we continued our analysis only with the activated fraction.

KEGG pathway analysis was performed only for aUCP and aPRP samples. The analysis revealed that among others, PI3K-Akt signaling pathway was shared by proteins detected in both samples. Hippo pathway only appeared in aUCP fraction while MAPK and Rap1pathways, in aPRP fractions (Figure 2B).

Growth factors, interleukins and chemokines in plasma samples

The results of the arrays revealed a statistically higher concentration (pg/mL) of several growth factors in both aUCP(*) and naUCP(**) fractions when compared with aPRP. These growth factors were TGFβ (P=0.0048*; P=0.0024**), kit ligand or SCF (P=0.0001*; P<0.0001**), PDGFBB (P=0.0008*; P=0.0024**), HGF (P=0.0005*; P=0.0003**), and VEGFD (P=0.0011*; P=0.0006**) (Figure 2C). From all the cytokines and chemokines studied, we detected IL2, IL7, IL15, IL18, eotaxin, leukemia inhibitory factor (LIF), monocyte chemoattractant protein

1 (MCP1) and SDF1α in all samples. However, only IL1-RA (*P*=0.0060*; *P*=0.0010**) and IL15 (*P*=0.0026) presented statistically differential results; to note that IL15 was the only molecule with a significantly higher concentration in aPRP (Figure 2C). A complete list of the analyzed molecules and the values obtained can be found in Supplemental Table 1.

Increased in vitro cell proliferation and migration after treating cells with plasma

To measure viable cell proliferation rates, we first performed MTS assays. The preliminary tests using ICE7 cells revealed that the highest rate was found in the presence of 1% plasma in the culture media (*P*=0.0015) (Figure 3A) and reaffirmed the higher potential of aPRP (*P*=0.0034) to stimulate cell proliferation compared to aPPP (Figure 3B). These initial tests also reinforced the positive effect of the activation process, when comparing aPRPC (*P*=0.0171) and naPRPC with the No Treatment condition (Figure 3B). As seen on Figure 3B, aPRPC (fold change, FC = 1.20) seems to have a similar effect than aPRP (FC = 1.26), confirming that plasma from AS/EA patients is not affected.

Secondly, in the main proliferation assay using ICE7, proliferation rates from aPRP (*P*=0.0380) and aUCP (*P*=0.0042) conditions were significantly higher compared with the No Treatment condition. Furthermore, this increment was higher when applying aUCP (FC = 1.36) instead of aPRP (FC = 1.22) (Figure 3C). These results were reproducible when using primary stromal cells (hESCs). Cell proliferation was significantly incremented with the addition of aPRP (*P*=0.0394) and aUCP (*P*<0.0001) to the culture media. In this case, aPRP proliferation rate increased by a 1.30 fold change and aUCP, by 1.80 fold change (Figure 3D).

Regarding the wound healing assay, results appeared to generally corroborate these previous results, despite being not statistically significant. There was a noticeable higher trend to cover the initial gap (in % of gap closure 24 hours after the wound) when cells were treated with aPRP (42.20 %) or aUCP (49.40 %) in comparison with the No Treatment condition (38.77 %), using ICE7 (Figure 3E, upper part). This effect was also reproducible with hESCs where aPRP (50.78 %) and aUCP (53.69 %) seemed to induce a higher wound closure rate than the No Treatment condition (42.52 %) (Figure 3E, lower part).

In vivo increased expression of cell proliferation and endometrial markers after applying aPRP

A preliminary test performed in the animal model revealed that aPRP was likely promoting tissue regeneration. The Ki67 immunoassay, which evaluates the cell proliferation rate, showed an increased significant signal *(P*=0.0106) in the damaged horns when compared to the control ones from aPRP group (Figure 4A, left). Hoxa10, an important transcription factor for many genes involved in the endometrial function and development, measured by WB also showed a more intense signal in damaged versus control horns (Figure 4A, right), without being statistically significant.

Relative protein quantification in murine uterine horns revealed aUCP as the gold standard treatment

The SWATH-MS analysis of the right and left uterine horns (n=48) from all mice groups (No treatment, aPRP, naUCP and aUCP) revealed the presence of 2766 different tissue proteins. We performed a statistical analysis using 2 different approaches: firstly, we compared the damaged versus control horns in aPRP,

naUCP and aUCP groups separately, and secondly, the damaged horns in each group against damaged ones in the rest of the groups. A detailed list of the differentially expressed proteins (DEP) after performing both approaches is shown in Supplemental Table 2.

When we globally analyzed the abundance of proteins in both horns, the damaged and control group profiles were clearly distinguishable (Figure 4B). Interestingly, we found that the up-regulated proteins in the damaged horns of the aUCP group were implicated in different events related to tissue regeneration such as PI3K-Akt, TGFβ or JAK-STAT signaling pathways. These proteins were P85α (a subunit of phosphatidylinositol 3-kinase), 2aaa (Pr65 subunit of protein phosphatase 2A), Stat5a (a signal transducer and activator of transcription) and Rhoa (a small GTPase). To note that the up-regulated proteins in the damaged horns of the other groups, aPRP and aUCP, were not involved in the signaling pathways mentioned here.

When we only analyzed the damaged horns, proteins seemed to group depending on the treatment applied (Figure 4C). When analyzing these proteins in-depth, damaged horns from group C (aUCP) showed an up-regulation of Uba3 (NEDD8-activating enzyme E1 catalytic subunit), Thy1 (CD90 antigen), Rnh1 (ribonuclease inhibitor) and Atpo (mitochondrial membrane ATP synthase). These last 2 proteins, together with Ppp1ca (protein phosphatase) and Golga2 (Golgin subfamily A member 2), were upregulated in group D (aPRP). Atp1b3 (a subunit of a sodium/potassium-transporting ATPase) was up-regulated in group B (naUCP) and Cklf6 (member of the chemokine-like factor superfamily) and Ndkb (nucleoside diphosphate kinase B), in group A (No Treatment).

WB analysis of several of these DEP, in both approaches, corroborated the regulation pattern of these proteins (Supplemental Figure 1). The selected proteins were Cklg6, Golga2, Uba3, Atp1b3, the cytosolic Fe-S cluster assembly factor Nubp2, the tubulin γ2 (Tbg2) and the transmembrane protein 256 (Tmem256).

DISCUSSION

Along this study, we reinforced the regenerative potential of plasma depending on its specific composition or source. This was done via assessing endometrial cell proliferation and migration in *in vitro* assays and tissue regeneration in an AS murine model. We also demonstrated via proteomic analysis the superior potential of the UCB over the adult blood as a source of regenerative plasma.

The main goal in patients affected with either AS or EA is to regenerate the endometrial tissue, restoring its normal proliferation rate and thickness. Thus, it is necessary to trigger the complex regeneration process which includes distinct events such as angiogenesis, cell recruitment, matrix deposition and inflammation (47). We postulate here that the presence and concentration of several growth factors, chemokines and cytokines change with the age of the plasma and PRP could play a role in these kinds of processes. We also demonstrated that the (adult or UCB) origin affected the concentration of some of these molecules. Among these, a potent mitogen (HGF) and other growth factors involved in cell chemotaxis and proliferative activities (PDGFBB, SCF), events involving angiogenesis (TGFβ, VEGFD) and the inflammatory response (IL1-RA), had a statistically significant higher concentration in UCP (in both a/na) (29,30), providing a higher regenerative ability, while IL2, IL7 and IL15 were more concentrated in adult PRP. The increased concentration of these

pro-inflammatory cytokines could be explained by the immune immaturity of the UCB (29,48), a characteristic that, added to the fact that plasma is an acellular blood fraction, completely minimize any kind of immunological issue, mainly a rejection reaction when using UCB (49). These results complement previous studies where a detrimental effect of aging in plasma was shown (32,50). Castellano *et al.* demonstrated that UCP could regenerate hippocampal function in aged mice (32) better than adult plasma via specific key factors. These proteins were also detected only (or with a higher score) in the UCP samples, corroborating the results of in this study. The *in silico* functional analysis of these plasma proteins showed different signaling pathways involved in cell proliferation, differentiation and migration, such as the PI3K-Akt pathway, that could be triggering the regeneration processes. The identification of these pathways also correlates with our *in vitro* results where an increase in cell proliferation and migration rates was seen when adding PRP to the medium, with UCP outperforming the other groups.

Some studies already demonstrated the beneficial effect of adult PRP over animal models with induced uterine damage (24,25), however none included the younger UCP as done in this study. In our AS murine model, after a deep analysis of the protein patterns of the uterine tissue, we established that aUCP produced major changes in the protein abundance tissue pattern. The functional analysis revealed that the up-regulated proteins in the aUCP group were mainly involved in the regulation of angiogenesis and mitotic cell cycle: Uba3, described as essential for NEDD8-mediated neddylation that is required for normal human endometrial function (51); Thy1/CD90, a well-known endometrial stromal cell marker (2); and, Rini, a regulator of neovascularization that has also

been described as down-regulated in endometrial glands in endometriotic versus healthy endometrium samples (52). Besides, when comparing the damaged versus the control uterine horns in the aUCP group, up-regulated proteins such as Stat5a (a mediator of cell response to SCF and other growth factors), were also involved in PI3K-Akt and JAK-STAT pathways, as the plasma proteins, but in further steps of the cascades.

Considering this study as pioneer in the use of umbilical cord blood plasma in the endometrial field even using pre-clinical murine models, we are aware about several limitations to this work. Since plasmas samples were not very easy to obtain, our sample size was small. Despite the wound healing assay is the most widely used, several restrictions such as injure/stress/non- proliferation processes affecting cell migration have been described after performing the scratch. Other options related to this issue should be further explored, either with longer exposure times or with other types of migration assays.

Conclusions

Given the specific mechanisms described above, it becomes apparent that PRP is a promising regenerative enhancer, especially when using UCB. Activated UCP revealed to be the best treatment in 3 different scenarios: analysis of plasma composition (higher concentrations of key molecules involved in pro-regenerative processes), *in vitro* evaluation of cell proliferation, and migration and uterine tissue analysis in an AS murine model. Nonetheless, despite that autologous PRP has already started to be used in human patients suffering from AS/EA (27,28,53–55), specific clinical studies are needed to reinforce the higher effectiveness of UCP versus adult PRP.

SUPPORT

This work was supported by grants CPII18/00002 (F.D.), CPI19/00149 (I.C.) and PI17/01039 (I.C.) from the Carlos III Health Institute, FPU18/06327 (E.F-H.) from the Spanish Ministry of Science and Innovation and by PROMETEO/2018/137 (L.Dm-G., A.P., I.C.) and ACIF/2017/117 (S.L-M.) from the Regional Valencian Ministry of Education.

ACKNOWLEDGMENTS

The authors express their sincere thanks to the Proteomic Service from the University of Valencia, especially to Oreto Antúnez and Luz Valero, and to all of the medical staff of IVIRMA clinics for their assistance in obtaining plasma and endometrium samples. In addition, the authors thank the statistical support received from Raquel Gavidia (SCSIE, University of Valencia) and Guillermo Mollá (IVI Foundation).

BIBLIOGRAPHY

1. Cervelló I, Gil-Sanchis C, Mas A, Delgado-Rosas F, Martínez-Conejero JA, Galán A, et al. Human endometrial side population cells exhibit genotypic, phenotypic and functional features of somatic stem cells. PLoS One 2010; 5:e10964.

2. Cervelló I, Mas A, Gil-Sanchis C, Peris L, Faus A, Saunders PTK, et al. Reconstruction of endometrium from human endometrial side population cell lines. PLoS One 2011; 6:e21221.

3. Sunkara SK, Khairy M, El-Toukhy T, Khalaf Y, Coomarasamy A. The effect of intramural fibroids without uterine cavity involvement on the outcome of IVF treatment: A systematic review and meta-analysis. Hum Reprod 2010; 25:418–29.

4. Myers EM, Hurst BS. Comprehensive management of severe Asherman syndrome and amenorrhea. Fertil Steril 2012; 97:160–4.

5. Zhao J, Zhang Q, Li Y. The effect of endometrial thickness and pattern measured by ultrasonography on pregnancy outcomes during IVF-ET cycles. Reprod Biol Endocrinol 2012; 10:100.

6. Conforti A, Alviggi C, Mollo A, De Placido G, Magos A. The management of Asherman syndrome: a review of literature. Reprod Biol Endocrinol 2013; 11:118.

7. Senturk LM, Erel CT. Thin endometrium in assisted reproductive technology. Curr Opin Obstet Gynecol 2008; 20:221-8.

8. Mahajan N, Sharma S. The endometrium in assisted reproductive

technology: How thin is thin? J Hum Reprod Sci 2016; 9:3–8.

9. Morelli SS, Rameshwar P, Goldsmith LT. Experimental Evidence for Bone Marrow as a Source of Nonhematopoietic Endometrial Stromal and Epithelial Compartment Cells in a Murine Model. Biol Reprod 2013; 89:1–7.

10. Zhao J, Zhang Q, Wang Y, Li Y. Uterine Infusion With Bone Marrow Mesenchymal Stem Cells Improves Endometrium Thickness in a Rat Model of Thin Endometrium. Reprod Sci 2015; 22:181–8.

11. Jing Z, Qiong Z, Yonggang W, Yanping L. Rat bone marrow mesenchymal stem cells improve regeneration of thin endometrium in rat. Fertil Steril 2014; 101:587–94.e3.

12. Cervelló I, Gil-Sanchis C, Santamaría X, Cabanillas S, Díaz A, Faus A, et al. Human CD133+ bone marrow-derived stem cells promote endometrial proliferation in a murine model of Asherman syndrome. Fertil Steril 2015; 104:1552–60.e1-3.

13. Gil-Sanchis C, Cervelló I, Khurana S, Faus A, Verfaillie C, Simón C. Contribution of different bone marrow-derived cell types in endometrial regeneration using an irradiated murine model. Fertil Steril 2015; 103:1596-1605.e1.

14. Santamaria X, Cabanillas S, Cervelló I, Arbona C, Raga F, Ferro J, et al. Autologous cell therapy with CD133+ bone marrow-derived stem cells for refractory Asherman's syndrome and endometrial atrophy: A pilot cohort study. Hum Reprod 2016; 31:1087–96.

15. Albanese A, Licata ME, Polizzi B, Campisi G. Platelet-rich plasma (PRP) in dental and oral surgery: From the wound healing to bone regeneration. Immun Ageing 2013; 10:23.

16. Leo MS, Kumar AS, Kirit R, Konathan R, Sivamani RK. Systematic review of the use of platelet-rich plasma in aesthetic dermatology. J Cosmet Dermatol 2015; 14:315–23.

17. Picard F, Hersant B, Bosc R, Meningaud JP. The growing evidence for the use of platelet-rich plasma on diabetic chronic wounds: A review and a proposal for a new standard care. Wound Repair Regen 2015; 23:638–43.

18. Marx RE. Platelet-Rich Plasma (PRP): What Is PRP and what is not PRP? What is PRP? What is PRP in relation to recombinant growth factors? Implant Dent 2001; 10:225–8.

19. Anitua E, Prado R, Nurden A, Nurden P. Characterization of Plasma Rich in Growth Factors (PRGF): Components and Formulations. In: Anitua E, Cugat R, Sánchez M, eds. Platelet rich plasma in orthopaedics and sports medicine. Springer 2018; 29-46.

20. Gargett CE, Chan RWS, Schwab KE. Hormone and growth factor signaling in endometrial renewal: Role of stem/progenitor cells. Mol Cell Endocrinol 2008; 288:22–9.

21. Matsumoto H, Nasu K, Nishida M, Ito H, Bing S, Miyakawa I. Regulation of proliferation, motility, and contractility of human endometrial stromal cells by platelet-derived growth factor. J Clin Endocrinol Metab 2005; 90:3560–7.

22. Anitua E, de la Fuente M, Ferrando M, Quintana F, Larreategui Z, Matorras R, et al. Biological effects of plasma rich in growth factors (PRGF) on human endometrial fibroblasts. Eur J Obstet Gynecol Reprod Biol 2016; 206:125–30.

23. Aghajanova L, Houshdaran S, Balayan S, Manvelyan E, Irwin JC, Huddleston HG, et al. In vitro evidence that platelet-rich plasma stimulates cellular processes involved in endometrial regeneration. J Assist Reprod Genet 2018; 35:757–70.

24. Jang HY, Myoung SM, Choe JM, Kim T, Cheon YP, Kim YM, et al. Effects of autologous platelet-rich plasma on regeneration of damaged endometrium in female rats. Yonsei Med J 2017; 58:1195–203.

25. Kim JH, Park M, Paek JY, Lee W-S, Song H, Lyu SW. Intrauterine infusion of human Platelet-Rich Plasma improves endometrial regeneration and pregnancy outcomes in a murine model of Asherman's syndrome. Front Physiol 2020; 11:105.

26. Tandulwadkar S, Naralkar M, Surana A, Selvakarthick M, Kharat A. Autologous intrauterine platelet-rich plasma instillation for suboptimal endometrium in frozen embryo transfer cycles: A pilot study. J Hum Reprod Sci 2017; 10:208–12.

27. Farimani M, Bahmanzadeh M, Poorolajal J. A new approach using autologous platelet-rich plasma to treat infertility and to improve population replacement rate. J Res Health Sci 2016; 16:172–3.

28. Zadehmodarres S, Salehpour S, Saharkhiz N, Nazari L. Treatment of thin endometrium with autologous platelet-rich plasma: A pilot study. J Bras

Reprod Assist 2017; 21:54–6.

29. Ehrhart J, Sanberg PR, Garbuzova-Davis S. Plasma derived from human umbilical cord blood: Potential cell-additive or cell-substitute therapeutic for neurodegenerative diseases. J Cell Mol Med 2018; 22:6157–66.

30. Murphy MB, Blashki D, Buchanan RM, Yazdi IK, Ferrari M, Simmons PJ, et al. Adult and umbilical cord blood-derived platelet-rich plasma for mesenchymal stem cell proliferation, chemotaxis, and cryo-preservation. Biomaterials 2012; 33:5308–16.

31. Parazzi V, Lazzari L, Rebulla P. Platelet gel from cord blood: A novel tool for tissue engineering. Platelets 2010; 21:549–54.

32. Castellano JM, Mosher KI, Abbey RJ, McBride AA, James ML, Berdnik D, et al. Human umbilical cord plasma proteins revitalize hippocampal function in aged mice. Nature 2017; 544:488–92.

33. Bae SH, Jo A, Park JH, Lim CW, Choi Y, Oh J, et al. Bioassay for monitoring the anti-aging effect of cord blood treatment. Theranostics 2019; 9:1–10.

34. National Library of Medicine (US). Identifier NCT02134132. Utilization of Platelet Gel for Treatment of Diabetic Foot Ulcers. Available at: https://clinicaltrials.gov/ct2/show/NCT02134132?term=NCT02134132&draw=2&rank=1 Accessed April 29, 2020.

35. National Library of Medicine (US). Identifier NCT02389010. Clinical Efficacy of Platelet Gel From Cord Blood for the Treatment of Diabetic Foot Ulcers. Available at:

https://clinicaltrials.gov/ct2/show/NCT02389010?term=NCT02389010&draw=2&rank=1 Accessed April 29, 2020.

36. National Library of Medicine (US). Identifier NCT03084861. A Clinical Trial to Asses Efficacy and Safety of Cord Blood Eye Drops in Neurotrophic Keratopathy. Available at: https://clinicaltrials.gov/ct2/show/NCT03084861?term=NCT03084861&draw=2&rank=1 Accessed April 29, 2020.

37. Mateos J, Carneiro I, Corrales F, Elortza F, Paradela A, del Pino MS, et al. Multicentric study of the effect of pre-analytical variables in the quality of plasma samples stored in biobanks using different complementary proteomic methods. J Proteomics 2017; 150:109–20.

38. Simón C, Piquette G, Frances A, Polan M. Localization of interleukin-1 type I receptor and interleukin-1 beta in human endometrium throughout the menstrual cycle. J Clin Endocrinol Metab 1993; 77:549–55.

39. Perez-Patiño C, Barranco I, Parrilla I, Valero ML, Martinez EA, Rodriguez-Martinez H, et al. Characterization of the porcine seminal plasma proteome comparing ejaculate portions. J Proteomics 2016; 142:15–23.

40. Carbon S, Douglass E, Dunn N, Good B, Harris NL, Lewis SE, et al. The Gene Ontology resource: 20 years and still GOing strong. Nucleic Acids Res 2019; 47:D330–8.

41. Kanehisa M, Goto S, Sato Y, Furumichi M, Tanabe M. KEGG for integration and interpretation of large-scale molecular data sets. Nucleic Acids Res 2012; 40:D109–14.

42. Raudvere U, Kolberg L, Kuzmin I, Arak T, Adler P, Peterson H, et al. g:Profiler: a web server for functional enrichment analysis and conversions of gene lists (2019 update). Nucleic Acids Res 2019; 47:W191–8.

43. Warde-Farley D, Donaldson SL, Comes O, Zuberi K, Badrawi R, Chao P, et al. The GeneMANIA prediction server: Biological network integration for gene prioritization and predicting gene function. Nucleic Acids Res 2010; 38:W214–20.

44. Zou H, Hastie T. Regularization and variable selection via the elastic net. J R Stat Soc Ser B Stat Methodol 2005; 67:301–20.

45. Krafts KP. Tissue repair: The hidden drama. Organogenesis 2010; 6:225-33.

46. Zhao M, Rotgans B, Wang T, Cummins SF. REGene: A literature-based knowledgebase of animal regeneration that bridge tissue regeneration and cancer. Sci Rep 2016; 6:23167.

47. Eming SA, Martin P, Tomic-Canic M. Wound repair and regeneration: Mechanisms, signaling, and translation. Sci Transl Med 2014; 6:265sr6.

48. Wang M, Yang Y, Yang D, Luo F, Liang W, Guo S, et al. The immunomodulatory activity of human umbilical cord blood-derived mesenchymal stem cells in vitro. Immunology 2009; 126:220–32.

49. Solves P, Carpio N, Balaguer A, Romero S, Iacoboni G, Gómez I, et al. Platelets does not influence the clinical outcome of patients undergoing autologous haematopoietic stem cell transplantation. Blood transfus 2015;

13:411-6.

50. Lehallier B, Gate D, Schaum N, Nanasi T, Lee SE, Yousef H, et al. Undulating changes in human plasma proteome profiles across the lifespan. Nat Med 2019; 25:1843–50.

51. Liao Y, Jiang Y, He H, Ni H, Tu Z, Zhang S, et al. NEDD8-mediated neddylation is required for human endometrial stromal proliferation and decidualization. Hum Reprod 2015; 30:1665–76.

52. Stephens AN, Hannan NJ, Rainczuk A, Meehan KL, Chen J, Nicholls PK, et al. Post-translational modifications and protein-specific isoforms in endometriosis revealed by 2D DIGE. J Proteome Res 2010; 9:2438–49.

53. Chang Y, Li J, Chen Y, Wei L, Yang X, Shi Y, et al. Autologous platelet-rich plasma promotes endometrial growth and improves pregnancy outcome during in vitro fertilization. Int J Clin Exp Med 2015; 8:1286–90.

54. Chang Y, Li J, Wei LN, Pang J, Chen J, Liang X. Autologous platelet-rich plasma infusion improves clinical pregnancy rate in frozen embryo transfer cycles for women with thin endometrium. Medicine (Baltimore) 2019; 98:e14062.

55. Molina AM, Sánchez J, Sánchez W, Vielma V. Platelet-rich plasma as an adjuvant in the endometrial preparation of patients with refractory endometrium. J Bras Reprod Assist 2018; 22:42–8.

FIGURE LEGENDS

Figure 1. Study design. (A) Platelet-rich plasma (PRP) preparation procedure from peripheral blood. Once isolated, it was activated (if necessary) using 5% of $CaCl_2$ 0.1M, aliquoted and stored at -80ºC. **(B)** Overview of the different assays and analysis performed using PRP from 3 different sources: commercial plasma from umbilical cord blood, 4 different Asherman's syndrome (AS)/Endometrial Atrophy (EA) patients and a control patient (healthy). Briefly, all plasmas were analyzed by LC-MS/MS and multiplex protein assays and used for 2 different *in vitro* assays (MTS and wound healing) using 2 different human endometrial stromal cell types (from a stem cell line and from primary culture) and for an animal model (mice uterine horns were analyzed by SWATH-MS proteomic procedure and by several protein assays).

Figure 2. Composition analysis of plasmas. (A) Venn diagram showing the number of common proteins between the activated and the non-activated fraction in UCP and the proteins present in all aPRP samples. **(B)** Venn diagram showing the shared KEGG pathways among the proteins detected by LC/MSMS in the aUCP and aPRP. **(C)** Multiplex protein assays results for cytokines, chemokines and growth factors are also shown, for the different samples analyzed. Data are presented as mean + standard deviation (SD). **P*<0.05 in aUCP vs aPRP; ***P*<0.05 in naUCP vs aPRP; ł*P*<0.05 in aPRP vs UCP(a/na).

Figure 3. *In vitro* assays: cell proliferation and migration assays. (A) Assessment of optimal concentration to supplement culture media. **(B)** Proof-of-concept MTS (proliferation assay) results in ICE7 line: comparison of cell proliferation between aPRP and aPPP fractions and activated and non-

activated PRPC samples. **(C)** MTS results using human endometrial stromal stem cells (ICE7, n=3) and **(D)** human endometrial stromal cells (hESCs, n=10). **(E)** Wound healing (cell migration) assays results using ICE7 stem cell line (n=3) and hESCs (n=10). Data are presented as mean + standard deviation (SD). *P<0.05

Figure 4. *In vivo* assays: AS/EA murine model. (A) Proof-of-concept: after aPRP treatment, Ki67 immunostaining was performed in uterine tissue sections (20X magnification) and Hoxa10 western blot performed from protein extracts of uterine horns. Data are presented as median ± interquartile range (IQR). **(B)** Heatmap of SWATH-MS data showing protein presence between damaged and undamaged horns. Up-regulated proteins related to the KEGG pathways in the graphs below are highlighted in bold. The other proteins were also detected in the comparison among the 4 types of damaged horns and/or validated by Western blot. **(C)** Left: heatmap of SWATH-MS results after Elastic Net penalization comparing damaged horns from the 4 groups. Proteins related to pro-regenerative events are highlighted in bold. Right: network (GeneMania) showing the interactions among the differentially expressed proteins in the different groups. *P <0.05.

SUPPLEMENTAL FIGURES AND TABLES

Supplemental figure 1. Validation of Elastic Net regularization SWATH-MS results by Western Blot. (A) Western blot bands for one validated protein among the up-regulated ones in each of the groups (comparison between damaged horns from the 4 groups): Cklf6 (No Treatment), Golga2 (aPRP), Uba3 (aUCP) and At1b3 (naUCP). **(B)** Graph showing the relative area measurement (ImageJ software). **(C)** Western blot bands for 3 validated protein

(one down- and 2 up-regulated when comparing damaged versus control horns) in the aPRP group (comparison between both horns from naUCP, aUCP and aPRP groups): Nubp2 (down), Tubulin γ2 (up) and Tmem256 (up). **(D)** Graph showing the relative area measurement (ImageJ software). Data are presented as mean + standard deviation (SD). **P*<0.05. Narrows indicate the group (part B) or horn (part D) in which the protein expression value was higher.

SUPPLEMENTAL TABLES

Supplemental table 1. Multiplex protein assays results of the analyzed plasmas. Protein targets included in the multiplex assays and the concentration values detected in analyzed samples. Blue wells show those factors that were statistically significant among the umbilical cord samples and the adult samples.

Supplemental table 2. SWATH-MS statistics results. Enumeration, including the ElasticNet coefficient, of the statistically differentiated proteins when performing the intergroup comparison among all damaged horns and the intragroup comparison in the naUCP, aUCP and aPRP groups. In blue, coefficients above 1, which indicate up regulation of the protein.

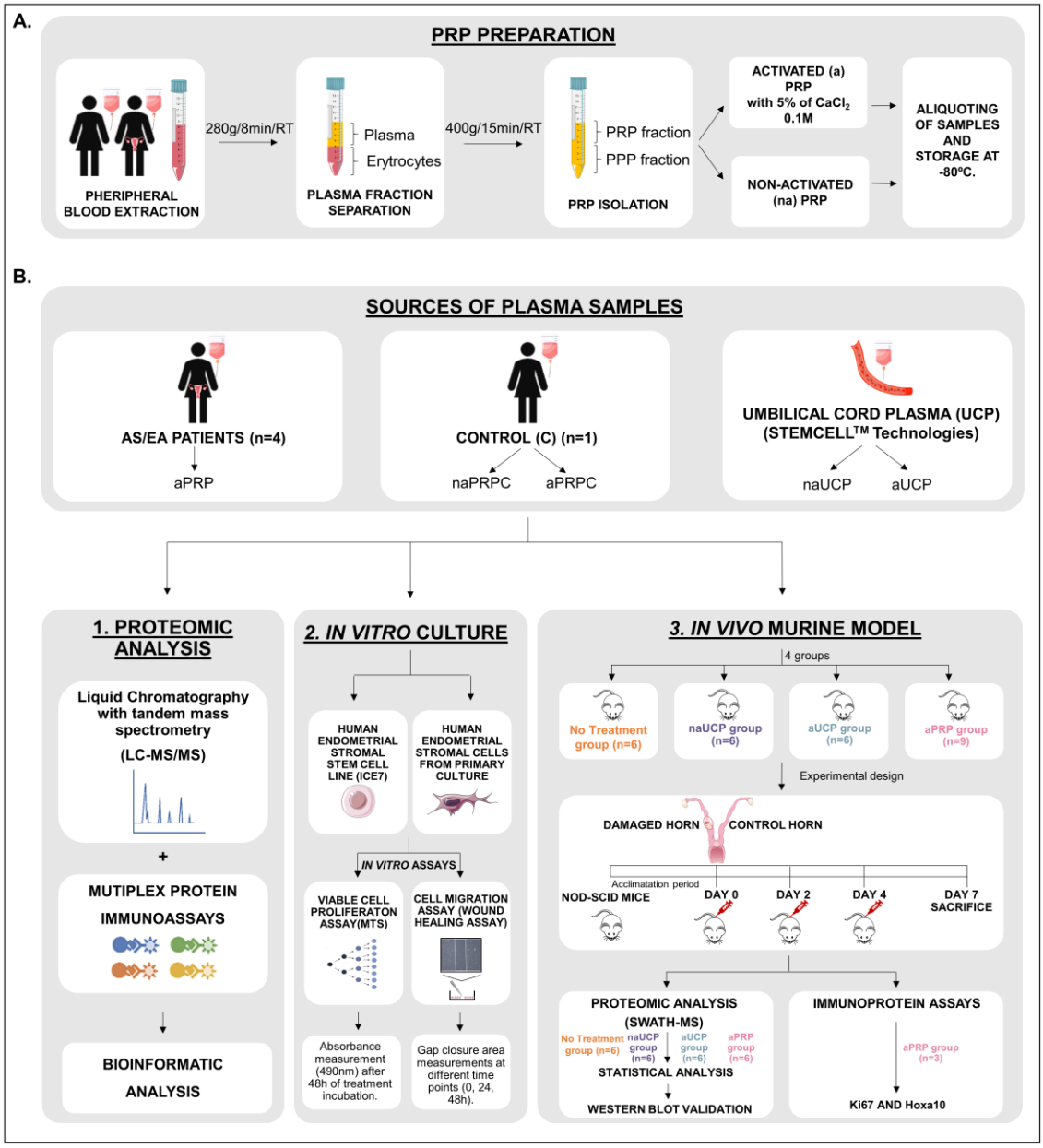
A.
PRP PREPARATION
PHERIPHERAL BLOOD EXTRACTION
280g/8min/RT
Plasma
Erytrocytes
PLASMA FRACTION SEPARATION
400g/15min/RT
PRP fraction
PPP fraction
PRP ISOLATION
ACTIVATED (a) PRP with 5% of CaCl2 0.1M
NON-ACTIVATED (na) PRP
ALIQUOTING OF SAMPLES AND STORAGE AT -80ºC.
B.
SOURCES OF PLASMA SAMPLES
AS/EA PATIENTS (n=4)
aPRP
CONTROL (C) (n=1)
naPRPC
aPRPC
UMBILICAL CORD PLASMA (UCP) (STEMCELL™ Technologies)
naUCP
aUCP
1. PROTEOMIC ANALYSIS
Liquid Chromatography with tandem mass spectrometry (LC-MS/MS)
+
MUTIPLEX PROTEIN IMMUNOASSAYS
BIOINFORMATIC ANALYSIS
2. IN VITRO CULTURE
HUMAN ENDOMETRIAL STROMAL STEM CELL LINE (ICE7)
HUMAN ENDOMETRIAL STROMAL CELLS FROM PRIMARY CULTURE
IN VITRO ASSAYS
VIABLE CELL PROLIFERATON ASSAY(MTS)
CELL MIGRATION ASSAY (WOUND HEALING ASSAY)
Absorbance measurement (490nm) after 48h of treatment incubation.
Gap closure area measurements at different time points (0, 24, 48h).
3. IN VIVO MURINE MODEL
4 groups
No Treatment group (n=6)
naUCP group (n=6)
aUCP group (n=6)
aPRP group (n=9)
Experimental design
DAMAGED HORN
CONTROL HORN
Acclimatation period
NOD-SCID MICE
DAY 0
DAY 2
DAY 4
DAY 7 SACRIFICE
PROTEOMIC ANALYSIS (SWATH-MS)
No Treatment group (n=6)
naUCP group (n=6)
aUCP group (n=6)
aPRP group (n=6)
STATISTICAL ANALYSIS
WESTERN BLOT VALIDATION
IMMUNOPROTEIN ASSAYS
aPRP group (n=3)
Ki67 AND Hoxa10

Figure 1

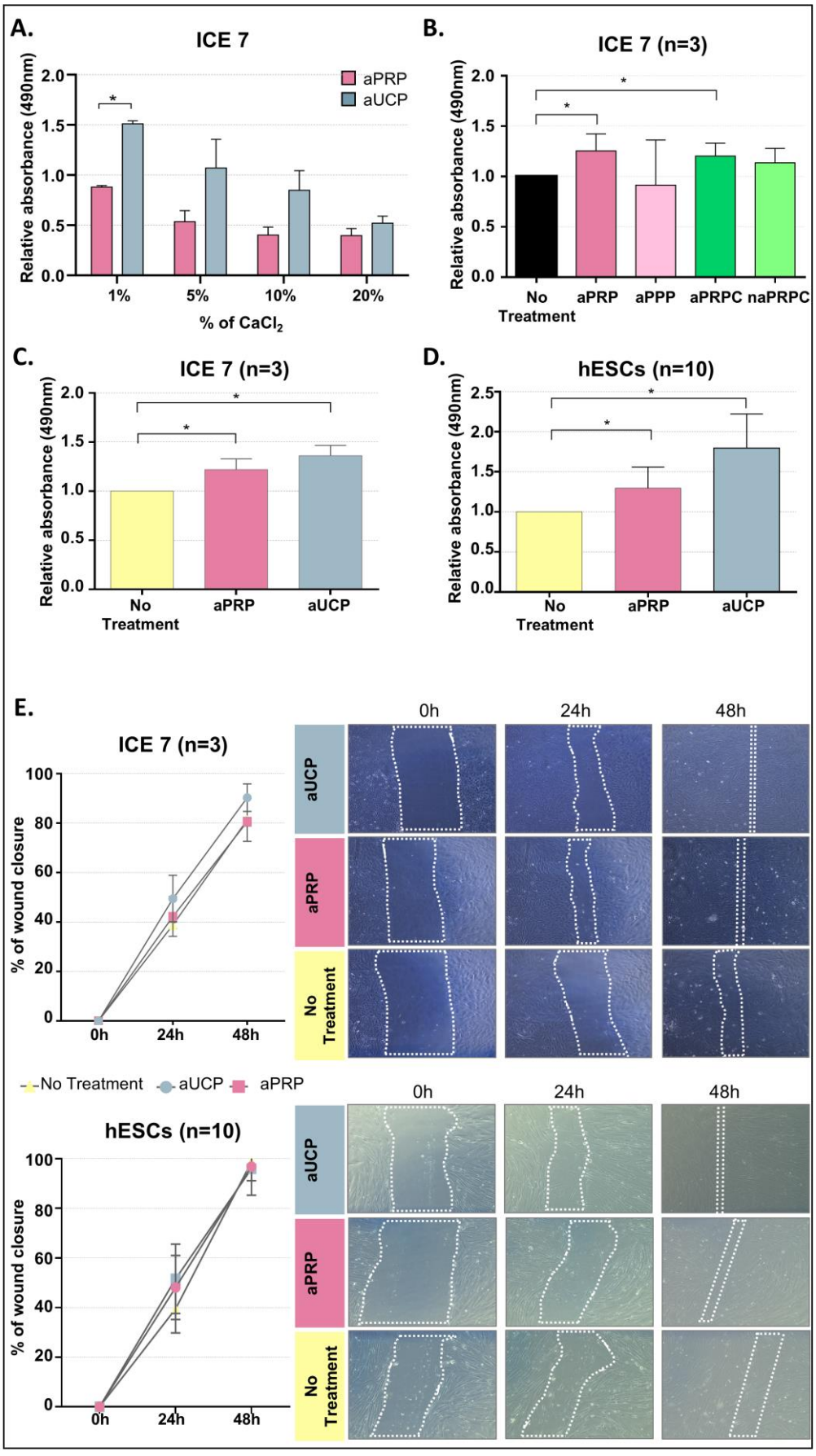
A.
ICE 7
aPRP
aUCP
Relative absorbance (490nm)
2.0
1.5
1.0
0.5
0.0
*
1%
5%
10%
20%
% of CaCl2
B.
ICE 7 (n=3)
Relative absorbance (490nm)
*
*
No Treatment
aPRP
aPPP
aPRPC
naPRPC
C.
ICE 7 (n=3)
Relative absorbance (490nm)
*
*
No Treatment
aPRP
aUCP
D.
hESCs (n=10)
Relative absorbance (490nm)
2.5
*
*
No Treatment
aPRP
aUCP
E.
ICE 7 (n=3)
% of wound closure
100
80
60
40
20
0
0h
24h
48h
0h
24h
48h
aUCP
aPRP
No Treatment
No Treatment
aUCP
aPRP
hESCs (n=10)
% of wound closure
0h
24h
48h
0h
24h
48h
aUCP
aPRP
No Treatment

Figure 2

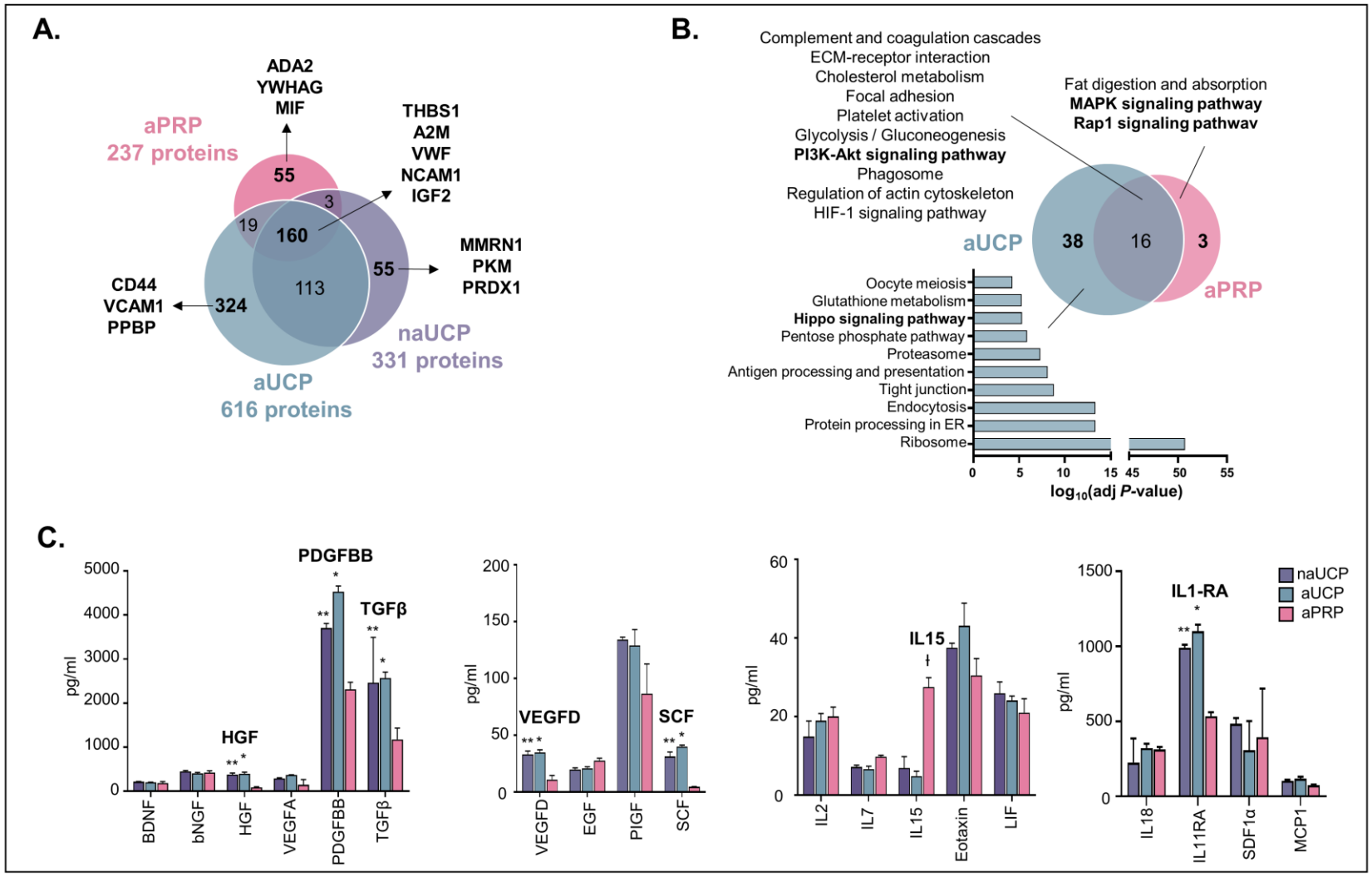
A.
ADA2
YWHAG
MIF
aPRP
237 proteins
55
3
19
160
THBS1
A2M
VWF
NCAM1
IGF2
MMRN1
PKM
PRDX1
55
CD44
VCAM1
PPBP
324
113
naUCP
331 proteins
aUCP
616 proteins
B.
Complement and coagulation cascades
ECM-receptor interaction
Cholesterol metabolism
Focal adhesion
Platelet activation
Glycolysis / Gluconeogenesis
PI3K-Akt signaling pathway
Phagosome
Regulation of actin cytoskeleton
HIF-1 signaling pathway
Fat digestion and absorption
MAPK signaling pathway
Rap1 signaling pathwav
aUCP
38
16
3
aPRP
Oocyte meiosis
Glutathione metabolism
Hippo signaling pathway
Pentose phosphate pathway
Proteasome
Antigen processing and presentation
Tight junction
Endocytosis
Protein processing in ER
Ribosome
0 5 10 15 45 50 55
log10(adj P-value)
C.
pg/ml
PDGFBB
TGFβ
HGF
BDNF
bNGF
HGF
VEGFA
PDGFBB
TGFβ
VEGFD
SCF
VEGFD
EGF
PIGF
SCF
IL15
IL2
IL7
IL15
Eotaxin
LIF
IL1-RA
IL18
IL11RA
SDF1α
MCP1
naUCP
aUCP
aPRP

Figure 3

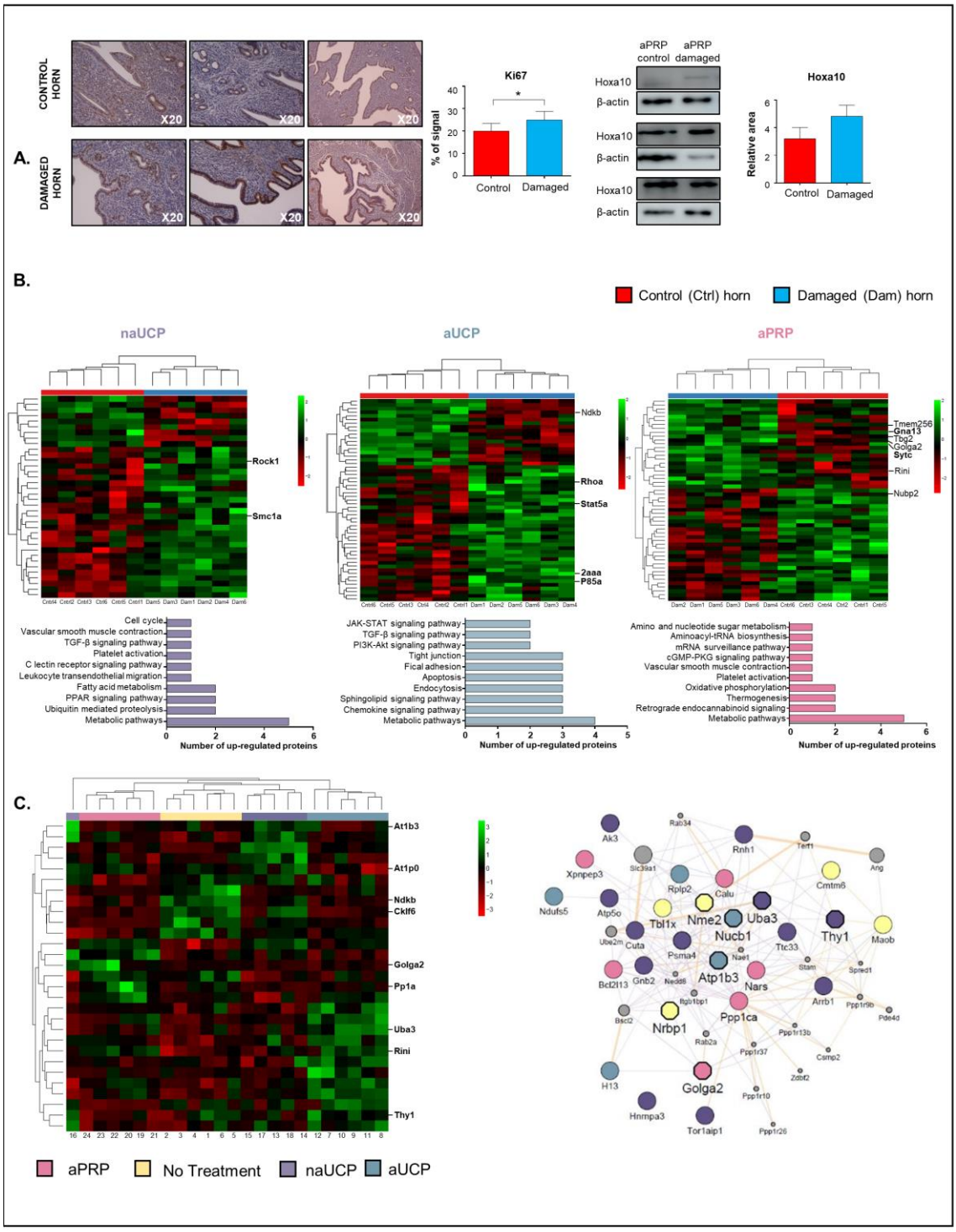
A.
CONTROL HORN
DAMAGED HORN
X20
Ki67
% of signal
Control
Damaged
aPRP control
aPRP damaged
Hoxa10
β-actin
Relative area
B.
Control (Ctrl) horn
Damaged (Dam) horn
naUCP
aUCP
aPRP
Rock1
Smc1a
Ndkb
Rhoa
Stat5a
2aaa
P85a
Tmem256
Gna13
Tbg2
Golga2
Sytc
Rini
Nubp2
Cell cycle
Vascular smooth muscle contraction
TGF-β signaling pathway
Platelet activation
C lectin receptor signaling pathway
Leukocyte transendothelial migration
Fatty acid metabolism
PPAR signaling pathway
Ubiquitin mediated proteolysis
Metabolic pathways
Number of up-regulated proteins
JAK-STAT signaling pathway
TGF-β signaling pathway
PI3K-Akt signaling pathway
Tight junction
Fical adhesion
Apoptosis
Endocytosis
Sphingolipid signaling pathway
Chemokine signaling pathway
Metabolic pathways
Number of up-regulated proteins
Amino and nucleotide sugar metabolism
Aminoacyl-tRNA biosynthesis
mRNA surveillance pathway
cGMP-PKG signaling pathway
Vascular smooth muscle contraction
Platelet activation
Oxidative phosphorylation
Thermogenesis
Retrograde endocannabinoid signaling
Metabolic pathways
Number of up-regulated proteins
C.
At1b3
At1p0
Ndkb
Ckif6
Golga2
Pp1a
Uba3
Rini
Thy1
aPRP
No Treatment
naUCP
aUCP
Ak3
Rab34
Rnh1
Tef1
Xpnpep3
Slc39a1
Ang
Rplp2
Calu
Cmtm6
Ndufs5
Atp5o
Tbl1x
Nme2
Uba3
Nucb1
Thy1
Maob
Ube2m
Cuta
Psma4
Naet
Ttc33
Stam
Spred1
Bcl2l13
Gnb2
Nedd8
Atp1b3
Nars
Arrb1
Ppp1r9b
Pde4d
Rgl1bp1
Bscl2
Nrbp1
Ppp1ca
Ppp1r13b
Rab2a
Ppp1r37
Csmp2
H13
Golga2
Zdbf2
Ppp1r10
Hnrnpa3
Tor1aip1
Ppp1r26

Figure 4

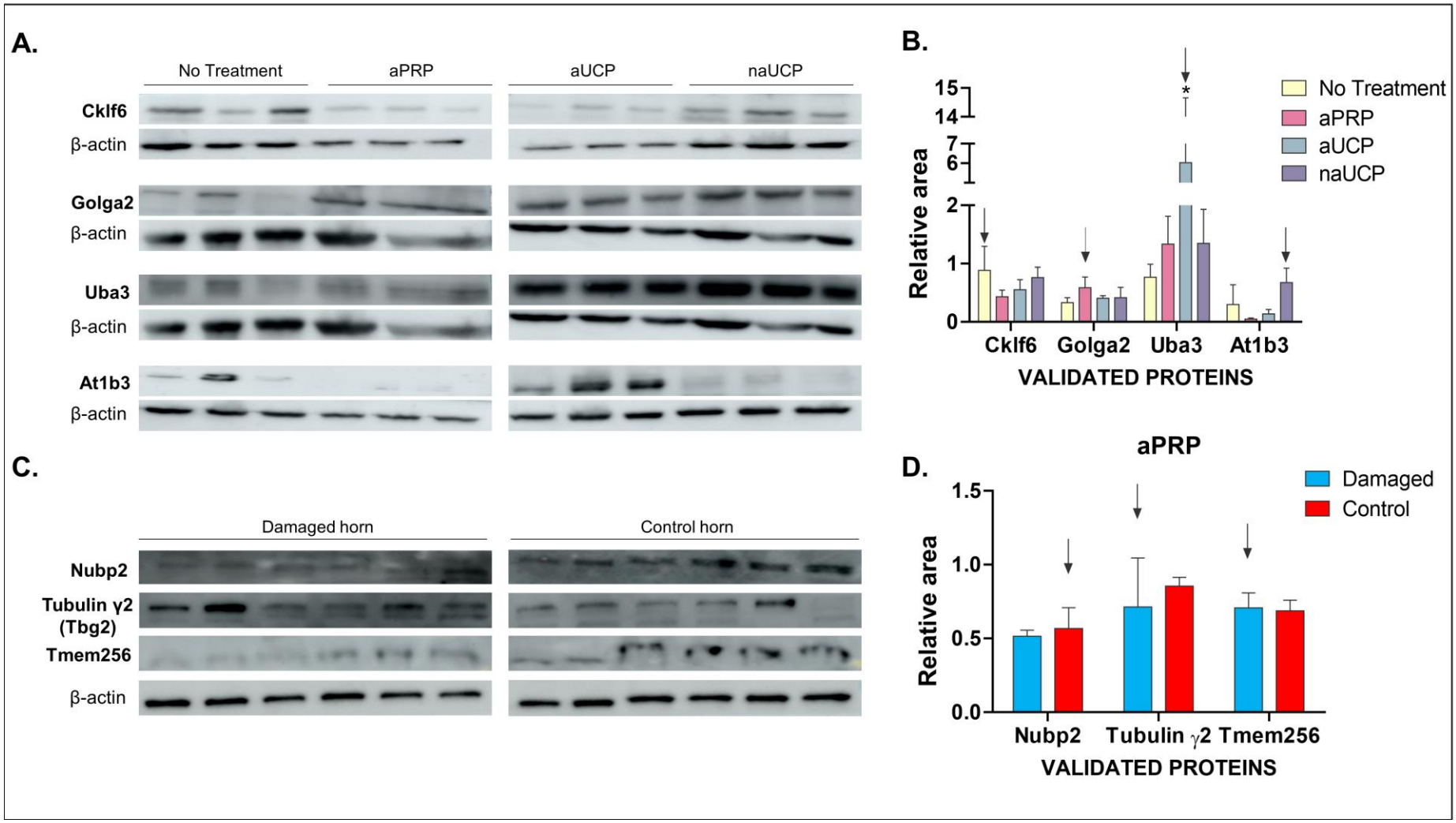

Supplemental Figure 1

Supplemental table 1

TARGET PROTEINS	COMPLETE NAME	aUCP	naUCP	aPRP
GM CSF	Granulocyte-macrophage colony-stimulating factor	UDL	UDL	UDL
IFN γ	Interferon gamma	UDL	UDL	UDL
IL1 β	Interleukin-1 beta	2.63	3.25	6.49
IL 12 p70	Interleukin-12, p70	UDL	UDL	UDL
IL13	Interleukin-13	17.65	UDL	UDL
IL18	Interleukin-18	225.04	322.31	312.57
IL2	Interleukin-2	14.93	18.99	20.06
IL4	Interleukin-4	UDL	UDL	UDL
IL5	Interleukin-5	18.88	6.30	UDL
IL6	Interleukin-6	UDL	UDL	UDL
TNF α	Tumor necrosis factor alpha	UDL	UDL	UDL
IL10	Interleukin-10	UDL	UDL	UDL
IL17A	Interleukin-17A	17.55	8.07	UDL
IL21	Interleukin-21	UDL	UDL	UDL
IL22	Interleukin-22	UDL	UDL	UDL
IL23	Interleukin-23	UDL	UDL	UDL
IL27	Interleukin-7	UDL	UDL	UDL
IL9	Interleukin-9	UDL	UDL	UDL
IFN α	Interferon alpha	UDL	UDL	UDL
IL1 α	Interleukin-1 alpha	UDL	UDL	UDL
IL1RA	Interleukin-1 receptor type 1	991.07	1101.37	534.29
IL15	Interleukin-4	6.94	4.86	27.54
IL31	Interleukin-31	UDL	UDL	UDL
IL7	Interleukin-7	7.19	6.69	9.83
TNF beta	Lymphotoxin-alpha	NA	NA	NA
eotaxin	Eotaxin	37.54	43.13	33.23
gro alpha/KC	Growth-regulated alpha protein	UDL	UDL	UDL
IL8	Interleukin-8	UDL	UDL	UDL
IP10	C-X-C motif chemokine 10	UDL	50.82	60.03
MCP1	C-C motif chemokine 2	104.83	118.20	74.71
MIP1 α	C-C motif chemokine 3	UDL	UDL	UDL
MIP1 β	C-C motif chemokine 4	UDL	UDL	UDL
RANTES	Regulated on Activation, Normal T Cell Expressed and Secreted, C-C motif chemokine 5	NA	NA	NA
SDF1 α	Stromal cell-derived factor 1	483.64	308.48	588.13
BDNF	Brain-derived neurotrophic factor	217.21	205.15	425.96
b NGF	Beta-nerve growth factor	311.38	308.40	756.45

EGF	Epidermal growth factor	19.76	20.95	63.87
FGF2	Fibroblast growth factor 2	9.27	UDL	UDL
HGF	Hepatocyte growth factor receptor	382.79	398.94	87.56
LIF	Leukemia inhibitory factor	25.95	24.16	25.86
PDGF BB	Platelet-derived growth factor subunit B	3702.54	4523.90	2312.27
PIGF	Phosphatidylinositol-glycan biosynthesis class F protein	134.13	128.94	160.93
SCF	Kit ligand	31.25	40.13	6.84
VEGF A	Vascular endothelial growth factor A	291.08	371.90	192.14
VEGF D	Vascular endothelial growth factor D	33.23	34.91	16.15
TGF β	Transforming growth factor beta	2449.06	441.12	1340.79

Supplemental table 2

Proteins	Coefficient naUCP	Coefficient aUCP
sp|Q9DB20|ATPO_MOUSE	4.16E-07	-4.92E-07
sp|Q9D6K7|TTC33_MOUSE	2.80E-05	2.47E-04
sp|Q9QXE7|TBL1X_MOUSE	1.99E-06	4.85E-07
sp|P01831|THY1_MOUSE	2.29E-07	6.66E-07
sp|Q9D8V0|HM13_MOUSE	7.59E-06	-1.64E-05
sp|Q9CZ69|CKLF6_MOUSE	4.47E-06	-8.90E-06
sp|Q9CQ89|CUTA_MOUSE	8.49E-07	-2.31E-06
sp|O35887|CALU_MOUSE	9.52E-06	-7.37E-07
sp|Q9WTP7|KAD3_MOUSE	7.63E-07	1.75E-06
sp|P97370|AT1B3_MOUSE	4.01E-07	-1.35E-07
sp|Q99LY9|NDUS5_MOUSE	1.60E-05	-4.40E-06
sp|P99027|RLA2_MOUSE	1.85E-05	-2.88E-06
sp|Q02819|NUCB1_MOUSE	1.44E-05	-3.23E-06
sp|Q8BP47|SYNC_MOUSE	-1.78E-05	-2.65E-06
sp|Q8BW75|AOFB_MOUSE	-6.82E-06	-2.75E-06
sp|Q01768|NDKB_MOUSE	-3.34E-07	-6.70E-07
sp|Q99J45|NRBP_MOUSE	-5.63E-07	8.71E-08
sp|Q91VI7|RINI_MOUSE	-4.35E-07	5.94E-07
sp|P59017|B2L13_MOUSE	-2.35E-05	4.43E-06
sp|Q8BWG8|ARRB1_MOUSE	-1.09E-05	1.78E-05
sp|P62137|PP1A_MOUSE	-1.84E-06	-1.06E-06
sp|Q921M4|GOGA2_MOUSE	-5.60E-06	-7.07E-06
sp|Q8BG05|ROA3_MOUSE	-1.32E-07	3.03E-07
sp|P62880|GBB2_MOUSE	-1.06E-06	1.66E-06
sp|Q9R1P0|PSA4_MOUSE	-1.11E-06	4.24E-06
sp|Q8C878|UBA3_MOUSE	-1.98E-06	4.23E-06
sp|Q8C1A5|THOP1_MOUSE	-2.56E-06	5.58E-06
sp|Q921T2|TOIP1_MOUSE	-2.87E-07	1.46E-05
sp|B7ZMP1|XPP3_MOUSE	-4.09E-05	9.74E-05

Coefficient aPRP	Coefficient No Treatment
3.63E-08	4.00E-08
-3.22E-04	4.77E-05
-4.56E-06	2.09E-06
-1.14E-06	2.41E-07
-7.84E-05	8.72E-05
-8.31E-06	1.27E-05
2.47E-06	-1.01E-06
1.58E-05	-2.46E-05
-1.98E-06	-5.32E-07
-2.25E-07	-4.09E-08
-9.91E-06	-1.67E-06
-6.77E-06	-8.83E-06
-1.47E-06	-9.66E-06
1.04E-05	1.01E-05
-8.29E-06	1.79E-05
-1.06E-06	2.06E-06
-1.39E-06	1.87E-06
7.91E-07	-9.49E-07
2.14E-05	-2.41E-06
3.59E-06	-1.05E-05
3.32E-06	-4.15E-07
1.83E-05	-5.59E-06
-1.31E-08	-1.57E-07
-1.89E-07	-4.13E-07
-1.91E-06	-1.23E-06
-7.11E-07	-1.54E-06
-9.06E-08	-2.94E-06
-9.26E-07	-1.34E-05
-4.01E-05	-1.65E-05

Proteins	Coefficient
sp|Q9JII5|DAZP1_MOUSE	8.68E-01
sp|P35282|RAB21_MOUSE	8.51E-01
sp|P14824|ANXA6_MOUSE	8.38E-01
sp|Q9D892|ITPA_MOUSE	5.41E-01
sp|Q99LY9|NDUS5_MOUSE	4.83E-01
sp|Q61074|PPM1G_MOUSE	4.71E-01
sp|Q8C460|ERI3_MOUSE	4.64E-01
sp|Q8C7R4|UBA6_MOUSE	2.61E-01
sp|P19973|LSP1_MOUSE	2.29E-01
sp|Q9D6Y7|MSRA_MOUSE	1.80E-01
sp|P36916|GNL1_MOUSE	1.73E-01
sp|P32020|NLTP_MOUSE	1.63E-01
sp|P61089|UBE2N_MOUSE	1.48E-01
sp|Q9CQM5|TXD17_MOUSE	1.42E-01
sp|Q3TLP5|ECHD2_MOUSE	1.18E-01
sp|Q9D6F9|TBB4A_MOUSE	1.05E-01
sp|Q80YR5|SAFB2_MOUSE	7.21E-02
sp|P97390|VPS45_MOUSE	5.94E-02
sp|Q9JKY0|CNOT9_MOUSE	4.76E-02
sp|Q9QYY8|SPAST_MOUSE	4.16E-02
sp|Q6P8J2|SAT2_MOUSE	3.07E-02
sp|Q9CQR6|PPP6_MOUSE	2.72E-02
sp|Q8VCN9|TBCC_MOUSE	2.24E-02
sp|Q9CU62|SMC1A_MOUSE	1.78E-02
sp|Q99PU5|ACBG1_MOUSE	1.42E-02
sp|P70335|ROCK1_MOUSE	1.08E-02
sp|Q80TL7|MON2_MOUSE	4.50E-03
sp|Q922P9|GLYR1_MOUSE	-1.61E-02
sp|O55028|BCKD_MOUSE	-1.98E-02
sp|Q6P2B1|TNPO3_MOUSE	-3.61E-02
sp|Q6NV83|SR140_MOUSE	-4.85E-02
sp|P49615|CDK5_MOUSE	-5.63E-02
sp|Q9ET01|PYGL_MOUSE	-2.20E-01
sp|Q9R0N0|GALK1_MOUSE	-3.73E-01
sp|Q8CHP8|PGP_MOUSE	-9.68E-01
sp|Q9ESZ8|GTF2I_MOUSE	-1.85E+00

Proteins	Coefficient
sp|Q8BG05|ROA3_MOUSE	1.19E+00
sp|Q76MZ3|2AAA_MOUSE	6.66E-01
sp|Q9CZD3|GARS_MOUSE	4.28E-01
sp|Q8K1M6|DNM1L_MOUSE	4.08E-01
sp|P50544|ACADV_MOUSE	3.79E-01
sp|P56399|UBP5_MOUSE	3.76E-01
sp|Q8VCW8|ACSF2_MOUSE	3.31E-01
sp|P68368|TBA4A_MOUSE	3.16E-01
sp|Q91WQ3|SYYC_MOUSE	2.25E-01
sp|P08775|RPB1_MOUSE	1.75E-01
sp|Q9CWZ3|RBM8A_MOUSE	1.70E-01
sp|Q9ER88|RT29_MOUSE	1.59E-01
sp|Q9D880|TIM50_MOUSE	1.59E-01
sp|O08734|BAK_MOUSE	1.57E-01
sp|P53996|CNBP_MOUSE	1.52E-01
sp|P26450|P85A_MOUSE	1.36E-01
sp|P10107|ANXA1_MOUSE	1.20E-01
sp|Q9D379|HYEP_MOUSE	9.30E-02
sp|Q3U2P1|SC24A_MOUSE	6.88E-02
sp|P21958|TAP1_MOUSE	4.85E-02
sp|Q71FD7|FBLI1_MOUSE	4.83E-02
sp|Q9CR86|CHSP1_MOUSE	4.64E-02
sp|Q922L6|NELFD_MOUSE	4.35E-02
sp|Q8BI72|CARF_MOUSE	4.32E-02
sp|Q8K2B3|SDHA_MOUSE	3.78E-02
sp|P63242|IF5A1_MOUSE	3.77E-02
sp|P36552|HEM6_MOUSE	3.19E-02
sp|P42230|STA5A_MOUSE	2.71E-02
sp|Q8BWG8|ARRB1_MOUSE	2.58E-02
sp|P14824|ANXA6_MOUSE	2.53E-02
sp|Q8K3C3|LZIC_MOUSE	2.14E-02
sp|Q62523|ZYX_MOUSE	1.94E-02
sp|Q9QUI0|RHOA_MOUSE	1.37E-02
sp|P47968|RPIA_MOUSE	1.34E-02
sp|Q07113|MPRI_MOUSE	1.14E-02
sp|Q9Z2Q6|SEPT5_MOUSE	9.45E-03
sp|Q05186|RCN1_MOUSE	6.31E-03
sp|P31786|ACBP_MOUSE	-1.61E-03
sp|Q61789|LAMA3_MOUSE	-1.58E-02
sp|P60843|IF4A1_MOUSE	-1.92E-02
sp|P99026|PSB4_MOUSE	-2.81E-02
sp|Q9D8X2|CC124_MOUSE	-4.62E-02
sp|Q06185|ATP5I_MOUSE	-5.77E-02
sp|Q9D7B7|GPX8_MOUSE	-6.39E-02
sp|Q3UZ39|LRRF1_MOUSE	-7.65E-02
sp|Q921Y0|MOB1A_MOUSE	-1.19E-01
sp|Q9WV98|TIM9_MOUSE	-2.46E-01
sp|Q9R0P5|DEST_MOUSE	-3.09E-01
sp|P62309|RUXG_MOUSE	-3.96E-01

sp|Q8R016|BLMH_MOUSE	-4.26E-01
sp|Q60692|PSB6_MOUSE	-4.46E-01
sp|P56391|CX6B1_MOUSE	-4.63E-01
sp|Q01768|NDKB_MOUSE	-4.80E-01
sp|P63168|DYL1_MOUSE	-5.89E-01
sp|P48758|CBR1_MOUSE	-7.08E-01

Proteins	Coefficient
sp|A2ASQ1|AGRIN_MOUSE	5.22E-01
sp|Q921M4|GOGA2_MOUSE	1.68E-01
sp|Q9D0R2|SYTC_MOUSE	1.61E-01
sp|Q8K4L3|SVIL_MOUSE	1.30E-01
sp|Q8VCK3|TBG2_MOUSE	9.76E-02
sp|P27601|GNA13_MOUSE	8.94E-02
sp|P97470|PP4C_MOUSE	8.84E-02
sp|Q99KJ8|DCTN2_MOUSE	8.68E-02
sp|Q80ZJ1|RAP2A_MOUSE	8.27E-02
sp|P47934|CACP_MOUSE	7.14E-02
sp|Q91VW3|SH3L3_MOUSE	6.79E-02
sp|Q8VE47|UBA5_MOUSE	6.71E-02
sp|Q9JLI6|SCLY_MOUSE	6.31E-02
sp|Q8VCF0|MAVS_MOUSE	5.61E-02
sp|Q9CQ91|NDUA3_MOUSE	5.27E-02
sp|Q91VI7|RINI_MOUSE	4.65E-02
sp|Q8BWY3|ERF1_MOUSE	3.71E-02
sp|Q78XR0|TPC6A_MOUSE	3.30E-02
sp|Q9JK38|GNA1_MOUSE	3.22E-02
sp|Q9JMA1|UBP14_MOUSE	2.76E-02
sp|Q5F285|TM256_MOUSE	1.01E-02
sp|Q99JT9|MTND_MOUSE	7.72E-03
sp|O35683|NDUA1_MOUSE	9.12E-04
sp|P28076|PSB9_MOUSE	-1.50E-03
sp|P14131|RS16_MOUSE	-1.93E-03
sp|Q60766|IRGM1_MOUSE	-2.34E-03
sp|Q7TNP2|2AAB_MOUSE	-3.58E-03
sp|Q9CRC8|LRC40_MOUSE	-4.00E-03
sp|Q80Y17|L2GL1_MOUSE	-1.23E-02
sp|Q9DBG1|CP27A_MOUSE	-1.60E-02
sp|Q8JZM8|MUC4_MOUSE	-2.04E-02
sp|Q9D0R8|LSM12_MOUSE	-2.39E-02
sp|Q811D0|DLG1_MOUSE	-3.94E-02
sp|P09470|ACE_MOUSE	-7.97E-02
sp|Q8C7K6|PCYXL_MOUSE	-8.07E-02
sp|P61211|ARL1_MOUSE	-8.15E-02
sp|Q99LG2|TNPO2_MOUSE	-1.09E-01
sp|A2ABV5|MED14_MOUSE	-1.16E-01
sp|Q8R5F8|ES8L1_MOUSE	-1.19E-01
sp|Q62470|ITA3_MOUSE	-1.36E-01
sp|Q924K8|MTA3_MOUSE	-1.39E-01
sp|Q8BMG7|RBGPR_MOUSE	-1.54E-01
sp|Q9D8V0|HM13_MOUSE	-1.59E-01
sp|Q9R062|GLYG_MOUSE	-1.75E-01
sp|O35972|RM23_MOUSE	-1.82E-01
sp|P53810|PIPNA_MOUSE	-1.92E-01

sp|Q2EMV9|PAR14_MOUSE	-2.77E-01
sp|Q9R061|NUBP2_MOUSE	-2.98E-01
sp|Q9CQL5|RM18_MOUSE	-2.98E-01
sp|Q91V09|WDR13_MOUSE	-3.41E-01
sp|P84104|SRSF3_MOUSE	-3.65E-01
sp|Q61510|TRI25_MOUSE	-4.75E-01